Uncertainty relation for resolution in space, spatial frequency, and orientation optimized by two-dimensional visual cortical filters

John G. Daugman

Division of Applied Sciences, Harvard University, Cambridge, Massachusetts 02138

Received May 17, 1982; accepted February 12, 1985

Two-dimensional spatial linear filters are constrained by general uncertainty relations that limit their attainable information resolution for orientation, spatial frequency, and two-dimensional (2D) spatial position. The theoretical lower limit for the joint entropy, or uncertainty, of these variables is achieved by an optimal 2D filter family whose spatial weighting functions are generated by exponentiated bivariate second-order polynomials with complex coefficients, the elliptic generalization of the one-dimensional elementary functions proposed in Gabor's famous theory of communication [J. Inst. Electr. Eng. 93, 429 (1946)]. The set includes filters with various orientation bandwidths, spatial-frequency bandwidths, and spatial dimensions, favoring the extraction of various kinds of information from an image. Each such filter occupies an irreducible quantal volume (corresponding to an independent datum) in a four-dimensional information hyperspace whose axes are interpretable as 2D visual space, orientation, and spatial frequency, and thus such a filter set could subserve an optimally efficient sampling of these variables. Evidence is presented that the 2D receptive-field profiles of simple cells in mammalian visual cortex are well described by members of this optimal 2D filter family, and thus such visual neurons could be said to optimize the general uncertainty relations for joint 2D-spatial–2D-spectral information resolution. The variety of their receptive-field dimensions and orientation and spatial-frequency bandwidths, and the correlations among these, reveal several underlying constraints, particularly in width/length aspect ratio and principal axis organization, suggesting a polar division of labor in occupying the quantal volumes of information hyperspace. Such an ensemble of 2D neural receptive fields in visual cortex could locally embed coarse polar mappings of the orientation–frequency plane piecewise within the global retinotopic mapping of visual space, thus efficiently representing 2D spatial visual information by localized 2D spectral signatures.

1. INTRODUCTION

The need for the visual nervous system to process efficiently a vast amount of information about the spatiotemporal world requires that image structure be extracted and represented with optimal economy. Both perceptual and neurophysiological vision research in the past two decades have been enlivened by debate over whether the fundamental character of early visual representation involves space-domain local feature detection[1–3] or more closely resembles a Fourier-like decomposition into spatial-frequency components.[4–7] As the polarization between these two views became articulated, and compelling evidence was marshaled on behalf of both theories, many investigators sought critical experiments[8–12] that would definitively resolve the issue. More recently, conciliatory voices[13–15] have affirmed that the debate was based on an illusory dichotomy because, once a visual mechanism is deemed linear, then its selectivities in either domain imply complementary ones in the other, and the crucial experimental results could be captured equally well by modest versions of either theory. The growing acceptance of the complementarity and appropriateness of both descriptions–one undulatory and the other localized–is reminiscent of the dissolving of the historic wave–particle debate in quantum physics. Probably the clearest voice of conciliation predates the spatial vision debate itself and was that of Dennis Gabor, whose classic 1946 monograph on the theory of communication[16] was pointed out to contemporary vision scientists by Marčelja[13] *vis-à-vis* interpretations of cortical simple cell receptive-field profiles.

Gabor's 1946 paper[16] formally proved by the use of Schwarz inequality arguments analogous to those underlying the indeterminacy relations of quantum mechanics that a signal's specificity simultaneously in time and frequency is fundamentally limited by a lower bound on the product of its bandwidth and duration. Reviewing the gradual recognition of this principle in the practical efforts of radio engineers in the 1920's, Gabor drew an interesting analogy: "... as the principle of conservation of energy emerged from the slowly hardening conviction of the impossibility of a *perpetuum mobile*, this fundamental principle of communication engineering arose from the refutation of ingenious attempts to break the as yet unformulated law" (Ref. 16, p. 429). Citing Heisenberg's and Weyl's related proofs, Gabor derived the uncertainty relation for information. He furthermore found the general family of signals that optimize this trade-off and thus achieve the theoretical lower limit of joint uncertainty in time and frequency, namely, all signals of the form $s(t) = \exp[-(t - t_0)^2/\alpha^2 + i\omega t]$, which in complex notation describes the modulation product of a sine wave with arbitrary frequency ω and a Gaussian envelope of arbitrary duration α occurring at epoch t_0. Gabor elaborated a quantum theory of information that consigns signals to regions of an information diagram whose coordinates are time and frequency and that has a quantal "grain," or minimal area (a product of frequency bandwidth times duration), dictated by the uncertainty principle; the quantal grain can be redistributed in shape but not reduced in area, and the general family of signals that achieve this smallest possible grain size are the Gaussian-modulated sinusoids. Finally, Gabor proposed representing arbitrary signals by a pseudoexpansion set of these elementary signals, which he termed "logons" in the infor-

0740-3232/85/071160-10$02.00

mation plane, indexed by all different frequencies of modulation and all different epochs of time.

Since 1980 several theorists concerned with spatial vision have recognized the suitability of Gabor's elementary signals as models for simple-cell receptive-field profiles,[13–15,17–20] provided that these cells behave essentially linearly, as several investigators have confirmed.[15,21–23] Typically two to five interleaved regions of excitatory and inhibitory influences weighted by a tapering envelope constitute the receptive-field profile of a simple cell, and Gabor signals with suitably chosen parameters invariably give a good fit to such spatial profiles. Particularly important for this synthesis was the discovery by Pollen and Ronner in 1981[17] of numerous pairs of adjacent simple cells matched in preferred orientation and spatial frequency but having a quadrature (90°) phase relationship within their common receptive-field area. Obviously the paramount significance of this finding is that a phase difference (optimally quadrature) is required between identical harmonic components in a frequency expansion, such as that envisaged in the Gabor scheme, even though such filters (while complete) are only pseudo-orthogonal. In any case, the well-established properties of simple-cell receptive fields as both localized yet undulatory now fit within a unified theoretical framework, and although the interpretive debate about what the Gabor-like representation achieves has hardly begun, at least the descriptive debate seems largely resolved into a synthesis of the two earlier views.

Today, however, this picture remains incomplete in several important respects. First, most applications of the Gabor framework to spatial vision have treated localization in one-dimensional (1-D) terms (namely, how position uncertainty Δx is related to spatial-frequency uncertainty Δu), in spite of the basic fact that a visual neuron's receptive field is localized in a *two*-dimensional (2D) spatial visual manifold. Second, the orientation selectivity of simple cells, which is perhaps their most salient tuning property, has not been explicitly analyzed in the uncertainty framework nor related to other tuning variables, such as spatial frequency and 2D spatial resolution. These two omissions in the theory are related to each other, and the analysis of either issue entails an analysis of the other. Filling in the missing dimension in the application of Gabor's (1D) scheme to (2D) spatial vision requires 2D filter theory[20] and is a major focus of this paper. Third, the role of several hidden constraints that do not play an essential part in the 2D Gabor scheme but that evidently are physiologically important limitations in the degrees of freedom will be analyzed, in the light of recently acquired empirical data on the 2D structure of simple-cell receptive-field profiles.

2. GENERAL UNCERTAINTY RELATION FOR TWO-DIMENSIONAL FILTERS

For a 1D complex signal or filter weighting function $f(x)$, a standard measure of effective width (Δx) is given by the square root of the variance, or second moment, of its energy distribution:

$$(\Delta x)^2 = \frac{\int_{-\infty}^{\infty} ff^* x^2 \mathrm{d}x}{\int_{-\infty}^{\infty} ff^* \mathrm{d}x},$$

where $f^*(x)$ is the complex conjugate of $f(x)$, so their product ff^* corresponds to the energy distribution. For simplicity the signal or filter here has been assumed to be origin centered ($x = 0$), and the denominator simply normalizes the measure of effective width to be independent of the amplitude of $f(x)$. If $f(x)$ has Fourier transform $F(\omega)$, whose effective bandwidth is also defined in terms of the analogous normalized second moment $(\Delta\omega)^2$ of its energy distribution FF^*, then the familiar[24] 1D uncertainty principle specifies a fundamental lower bound on the possible values of their product: $(\Delta x)(\Delta\omega) \geq 1/4\pi$.

For *2D* signals or filters $f(x, y)$ there are several possible generalizations of the concept of effective width, arising from the existence of not one but three Cartesian second moments for the (normalized and origin-centered) energy distribution $f(x, y)f^*(x, y)$:

$$\int_{-\infty}^{\infty}\int_{-\infty}^{\infty} x^2 f(x, y)f^*(x, y)\mathrm{d}x\mathrm{d}y,$$

$$\int_{-\infty}^{\infty}\int_{-\infty}^{\infty} y^2 f(x, y)f^*(x, y)\mathrm{d}x\mathrm{d}y,$$

$$\int_{-\infty}^{\infty}\int_{-\infty}^{\infty} xyf(x, y)f^*(x, y)\mathrm{d}x\mathrm{d}y.$$

The first two of these compute variance around the y axis and the x axis; the third (skew moment) computes asymmetry of the diagonals. It is known that any 2D distribution can always be rotated so that its skew moment is zero, and the angle of this rotation determines the distribution's principal axes. If a 2D distribution's principal axes correspond to the x axis and the y axis, then the second moment around each of these axes is the square of the distribution's effective width (Δx) or effective length (Δy), and the product of these two quantities $(\Delta x)(\Delta y)$ measures its effective area. Thus we may measure the effective (or occupied) area of a 2D signal or filter in terms of the product of its Cartesian second moments around the x and y axes, once it has been rotated so that these are its principal axes.

Analogous to the 1D uncertainty principle cited earlier, there are two 2D uncertainty principles constraining the effective width (Δx) and the effective length (Δy) of a 2D filter or signal $f(x, y)$ and the effective width (Δu) and the effective length (Δv) of its 2D Fourier transform $F(u, v)$. Regardless of the principal axes or any separability conditions, it can be shown[24] that for any arbitrary $f(x, y)$ centered on (x_0, y_0) whose 2D transform $F(u, v)$ is centered on (u_0, v_0), the following two uncertainty principles apply:

$$(\Delta x)(\Delta u) = \left[\frac{\int_{-\infty}^{\infty}\int_{-\infty}^{\infty} (x - x_0)^2 f(x, y)f^*(x, y)\mathrm{d}x\mathrm{d}y}{\int_{-\infty}^{\infty}\int_{-\infty}^{\infty} f(x, y)f^*(x, y)\mathrm{d}x\mathrm{d}y}\right]^{1/2}$$

$$\times \left[\frac{\int_{-\infty}^{\infty}\int_{-\infty}^{\infty} (u - u_0)^2 F(u, v)F^*(u, v)\mathrm{d}u\mathrm{d}v}{\int_{-\infty}^{\infty}\int_{-\infty}^{\infty} F(u, v)F^*(u, v)\mathrm{d}u\mathrm{d}v}\right]^{1/2} \geq \frac{1}{4\pi}, \quad (1a)$$

$$(\Delta y)(\Delta v) = \left[\frac{\int_{-\infty}^{\infty}\int_{-\infty}^{\infty}(y-y_0)^2 f(x,y) f^*(x,y)\,dx\,dy}{\int_{-\infty}^{\infty}\int_{-\infty}^{\infty} f(x,y) f^*(x,y)\,dx\,dy}\right]^{1/2}$$

$$\times \left[\frac{\int_{-\infty}^{\infty}\int_{-\infty}^{\infty}(v-v_0)^2 F(u,v) F^*(u,v)\,du\,dv}{\int_{-\infty}^{\infty}\int_{-\infty}^{\infty} F(u,v) F^*(u,v)\,du\,dv}\right]^{1/2} \geq \frac{1}{4\pi}. \quad (1b)$$

These two uncertainty principles are the fundamental conditions, from which follow certain other relations. The lower bounds in Eqs. (1a) and (1b) can be achieved only for certain functions $f(x, y)$ whose principal axes are parallel to x and y axes, and similarly for their transforms $F(u, v)$ and the u and v axes (although these two conditions do not imply each other). If these functions and transforms are rotated out of such axes, the products of effective widths will in general increase. If the principal axes do correspond, then each of the products $(\Delta x)(\Delta y)$ and $(\Delta u)(\Delta v)$ represents the effective area occupied by the signal or the filter in the corresponding 2D domain. It follows that the joint resolution that can be achieved by any 2D filter or signal in the two 2D domains, defined by these two occupied areas, is thus also constrained by a fundamental lower limit:

$$(\Delta x)(\Delta y)(\Delta u)(\Delta v) \geq 1/16\pi^2. \quad (2)$$

This new uncertainty principle, derived from the fundamental relations [Eqs. (1)], expresses the theoretical limit of joint 2D resolution in the two 2D domains.

3. JOINT TWO-DIMENSIONAL ENTROPY MINIMIZATION

It can be shown that the following family of functions $f(x, y)$ and their 2D Fourier transforms $F(u, v)$ achieve the lower bound in the above inequalities:

$$f(x,y) = \exp\{-\pi[(x-x_0)^2 a^2 + (y-y_0)^2 b^2]\} \times \exp\{-2\pi i[u_0(x-x_0) + v_0(y-y_0)]\},$$

$$F(u,v) = \exp\{-\pi[(u-u_0)^2/a^2 + (v-v_0)^2/b^2]\} \times \exp\{-2\pi i[x_0(u-u_0) + y_0(v-v_0)]\}. \quad (3)$$

Using the definitions for effective width and length in both domains [Eqs. (1a) and (1b)], one obtains

$$(\Delta x) = \frac{1}{2a\sqrt{\pi}}, \quad (\Delta y) = \frac{1}{2b\sqrt{\pi}},$$

$$(\Delta u) = \frac{a}{2\sqrt{\pi}}, \quad (\Delta v) = \frac{b}{2\sqrt{\pi}}.$$

Thus the joint 2D resolution for this family of 2D signals or filters, defined by the product of their occupied areas in the two 2D domains [Eq. (2)], achieves the theoretical limit of $1/16\pi^2$ regardless of the values of any of the parameters. Because of the analogy between this family of optimal 2D functions and Gabor's[16] time-varying signals, we shall call this the family of 2D Gabor functions.

The 2D Gabor function $f(x, y)$ [Eqs. (3)] is the product of an elliptical Gaussian with an aspect ratio (b/a) whose centroid is located at (x_0, y_0) times a complex exponential representing harmonic modulation with spatial frequency $(u_0^2 + v_0^2)^{1/2}$ and orientation $\arctan(v_0/u_0)$. The amplitude and the phase are specified by an assumed complex coefficient $Ae^{i\phi}$ multiplying Eqs. (3). In slightly more general form, both $f(x, y)$ and $F(u, v)$ would be defined as an exponentiated complete second-order bivariate polynomial

$$\exp[-(Ax^2 + Bxy + Cy^2 + Dx + Ey + F)],$$

where $B^2 < 4AC$ and D, E, and F are complex, but we have assumed for simplicity that $f(x, y)$ has been rotated so that its principal axes correspond to the x and y axes and therefore that the cross-product coefficient B is zero. It should be noted that 2D Gabor functions (1) have the same functional form in both 2D domains, as can be verified by applying the similarity theorem and the shift/modulation theorem to Eqs. (3); (2) are polar separable in neither domain; and (3) are Cartesian separable only in certain special cases.

Actual filter impulse-response functions and neural receptive-field profiles are real functions that can be regarded as projected out of such analytic functions, containing in quadrature both the even- and the odd-symmetric versions (cosine and sine parts). To obtain a physically meaningful quantity from the analytic function one can either simply take its real part or add to it its reflection in negative frequencies with conjugate amplitude. Gabor (Ref. 16, p. 432) discusses the relative merits of both methods; here we shall use the second method, and hence a real filter profile generated by Eqs. (3) will have a two-sided transform. For example, considering the two canonical quadrature cases, if $f(x, y)$ is in pure cosine phase, then its transform is $\frac{1}{2}\{F(u, v) + F(-u, -v)\}$; whereas, if $f(x, y)$ is in pure sine phase, then its transform is $\frac{1}{2}\{-iF(u, v) + iF(-u, -v)\}$. Intermediate phases represented by the appropriate mixture of these cases would generate filter profiles with neither symmetry nor antisymmetry.

A plot of a representative even-symmetric member of the 2D Gabor filter family, as originally proposed by Daugman,[20] is shown in Fig. 1. Referring to the parameters in Eqs. (3), this particular filter has $x_0 = y_0 = 0$, $u_0 = 0$, $v_0 = \pm 4$ cycles/deg, and $a^2 = b^2 = 16/\pi$ deg^{-2}. It should be noted that different

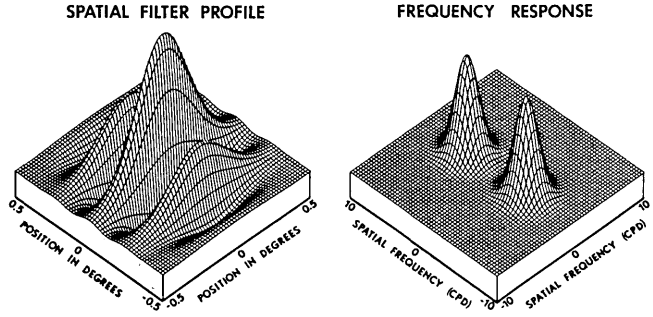

Fig. 1. An even-symmetric member of the family of 2D Gabor filters, with unity aspect ratio, and its 2D Fourier transform. Members of this filter family generated by Eqs. (3) have the sharpest possible joint resolution of information in the two 2D domains. The number of significant sidelobes in the space-domain profile inversely determines the filter's spatial-frequency bandwidth and orientation bandwidth; the spatial periodicity and orientation of the lobes specifies the filter's preferred spatial frequency and orientation. Different members of this optimal filter family are an excellent description of the 2D neural receptive fields found in the visual cortex, as illustrated in Fig. 3. CPD, cycles/degree. (From Ref. 20.)

Table 1. Corresponding Filter Properties in Space and Spectral Domains

2D Space Domain	2D Frequency Domain
Modulate filter envelope by spatial frequency ω_0 in wave-vector orientation θ_0	Position spectral centroid at Fourier plane coordinates (u_0, v_0), where $u_0 = \omega_0 \cos(\theta_0)$, $v_0 = \omega_0 \sin(\theta_0)$
Position filter centroid at space-domain coordinates (x_0, y_0)	Modulate transform by complex exponential having spectral frequency $(x_0^2 + y_0^2)^{1/2}$ and orientation $\arctan(y_0/x_0)$
Rotate filter through angle θ around origin of coordinates	Rotate transform through angle θ around origin of coordinates
Stretch (compress) filter in x direction by factor α	Compress (stretch) spectrum in u direction by factor α
Stretch (compress) filter in y direction by factor β	Compress (stretch) spectrum in v direction by factor β
Set envelope aspect ratio to λ	Set envelope aspect ratio to $1/\lambda$

choices for the values of these parameters would center the filter at different spatial locations (x_0, y_0) and give it different preferred spatial-frequency and orientation responses corresponding to centroid locations $(\pm u_0, \pm v_0)$, thus paving both 2D domains; and, depending on the bandwidth parameters a and b, a division of labor is created for favoring resolution in either the 2D space domain (for large values of a and b) or the 2D frequency domain (for small values of a and b), or, by mixing these cases, for favoring spatial resolution in one direction while favoring frequency or orientation resolution in the perpendicular direction. The joint effects of these operations for paving both 2D domains simultaneously and for specifying certain divisions of labor for resolution in the two domains, subject to the inescapable uncertainty relations, are summarized in Table 1.

The division of labor for different forms of resolution in the two 2D domains, for different members of the 2D Gabor filter family, is illustrated graphically in Fig. 2. The left-hand column represents a bird's-eye view of three even-symmetric filters, all having the same modulation spatial frequency and orientation but different width/length aspect ratios as indicated by the elliptical contours representing the $1/e$ amplitude level of the 2D envelopes. Similarly, the right-hand column of Fig. 2 represents the approximate $1/e$ amplitude contour for the two parts of the 2D Fourier transform of each of these filters. In the frequency domain the centroids of these filters all have the same locations, corresponding to peak spectral response at spatial frequency ω_0 in the vertical orientation as dictated by the pattern of modulation in the 2D space domain. But there are major differences in the three filters' resolutions for spatial frequency and orientation (the radial and angular dimensions of the contours in the frequency domain), which are seen to vary inversely with the two spatial dimensions.

Within the trigonometric limits of the construction in Fig. 2, approximate expressions are derived in the three right-hand panels for the corresponding filter's orientation half-bandwidth $\Delta\theta_{1/2}$ (in radians) and spatial-frequency bandwidth ΔF (in cycles/degree), in terms of the filter space-domain dimensions α and β (in degrees) and its modulation frequency ω_0 (in cycles/degree). For simplicity, the expressions for orientation bandwidth $\Delta\theta_{1/2}$ assume that these angles are small

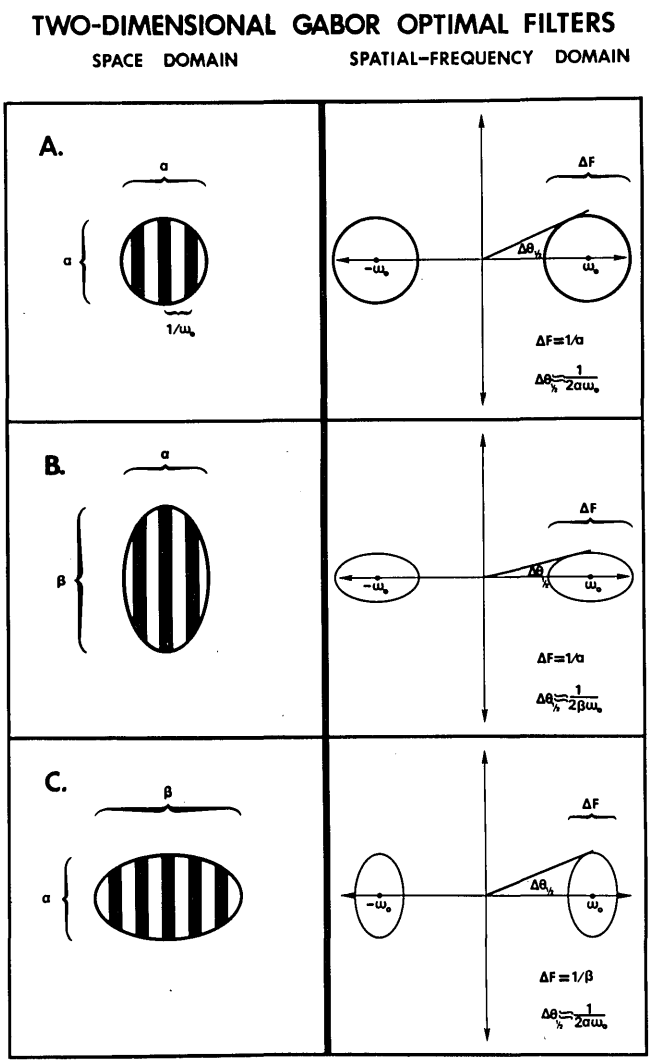

Fig. 2. Bird's-eye view of three members of the set of 2D Gabor optimal filters, all having the same preferred spatial frequency and orientation. The three pairs of panels illustrate the dependence of a filter's spatial-frequency bandwidth and orientation bandwidth on its space-domain envelope dimensions; its preferred frequency and orientation are independent of those dimensions. A, A circular filter envelope in the space domain is supported in the frequency domain by the sum of two circular regions whose centers correspond to the filter's modulation frequency and whose spatial-frequency bandwidth and orientation bandwidth are inversely related to the space-domain envelope diameter. B, Elongating the filter's receptive field in the direction parallel to its modulation sharpens its orientation bandwidth $\Delta\theta_{1/2}$ but has no effect on its spatial-frequency bandwidth ΔF. C, Elongating the field instead in the perpendicular direction sharpens its spatial-frequency bandwidth ΔF but has no effect on its orientation bandwidth $\Delta\theta_{1/2}$. Thus such filters can negotiate the inescapable trade-offs for resolution in different ways, attaining, for example, sharp spatial resolution in the y direction (at the expense of orientation selectivity) or sharp spatial resolution in the x direction (at the expense of spatial-frequency selectivity). Such a division of labor among filters, or visual neurons, permits the extraction of differentially resolved spatial–spectral information from the image. Always, however, for 2D Gabor filters the product of the 2D resolutions in the two 2D domains is the same and equals the theoretically attainable limit.

enough for $\sin(\theta)$ to be approximated by θ in radians. For filters with orientation half-bandwidths larger than about 30°, the expressions for $\Delta\theta_{1/2}$ should be replaced by arcsine arguments, and for still larger angles (corresponding to very short filters in the space domain) the orientation bandwidth and even the preferred orientation would start to depend dramatically on spatial frequency. The reciprocal scaling relations depicted graphically in Fig. 2 and the expressions for bandwidths in terms of space-domain properties can be derived from the 2D similarity theorem and the 2D modulation theorem, which relate the shapes and locations of the frequency-domain ellipses to the filter modulation and dimensions in the space domain.

A fundamental property captured in Fig. 2 is that the product of the occupied areas of any filter's analytic function in the two 2D domains is always independent of any dilation, translation, or modulation of its profile, and for 2D Gabor filters contained in the analytic functions of Eqs. (3) this product of occupied areas is always as small as it can possibly be, regardless of the values of any of the six parameters that generate the different filters in the family. A further property captured in Fig. 2 is that for different filters constrained to occupy the same total amount of 2D space-domain area (e.g., those in panels B and C), any gain in spatial-frequency resolution ΔF must be paid for by a loss in orientation resolution $\Delta\theta_{1/2}$; conversely, any gain in orientation resolution must be paid for by a loss in spatial-frequency resolution. This is because such filters that have a constant degree of 2D spatial resolution (integration area) must also occupy a fixed amount of area in the 2D frequency domain, and thus the frequency-domain ellipses in panels B and C are constant in area while their different shapes negotiate different trade-offs between $\Delta\theta_{1/2}$ and ΔF.

Finally, in analogy with Gabor's original information diagram (time–frequency plane), it is useful to think of these 2D spatial filters as located in a four-dimensional (4D) information hyperspace whose four orthogonal axes are x, y, u, and v (the 2D space and 2D frequency coordinates). In this geometrical interpretation of spatial information there is a 4D grain size, or minimal quantal volume, taken up by any spatial signal or filter, namely, $1/16\pi^2$ as noted in relation (2). Arbitrary 2D signals, such as actual images, could be efficiently represented by decomposition into the elementary signals defined in Eqs (3). Integrating the product of the image in question times each elementary signal results in a coefficient that specifies the amount of energy contained in each of these minimal quantal volumes that pack information hyperspace. Their minimal volume makes them the natural basis for image analysis in which both 2D spatial location and 2D spectral signature are recognized as important parameters. This completes our generalization of Gabor's information diagram and scheme for decomposition.

4. SIMPLE-CELL TWO-DIMENSIONAL RECEPTIVE-FIELD PROPERTIES IN STRIATE CORTEX

We turn now to empirical properties of simple cells in mammalian visual cortex in order to apply the 2D Gabor theoretical framework developed above for understanding their receptive-field profiles and the relationship between their selectivities for orientation and spatial frequency. Inasmuch as the preceding analysis is based on linear theory, the scope of an empirical characterization must be largely limited to linear neurons. Of the three classical categories of neurons found in the striate cortex as enumerated by Hubel and Wiesel,[1,2] namely, simple, complex, and hypercomplex cell types, only the simple cells are generally considered linear integrators of

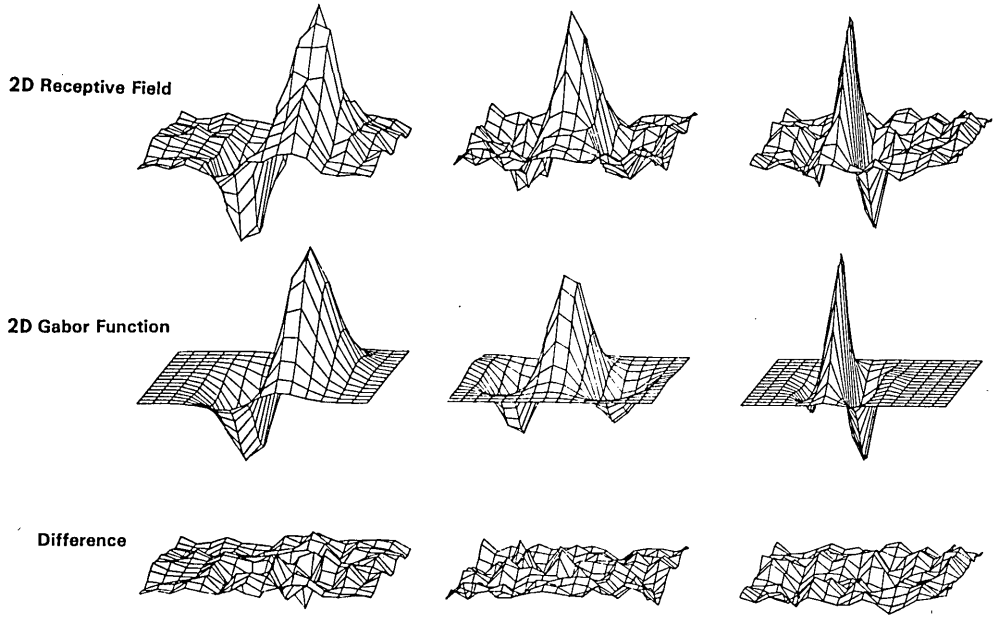

Fig. 3. Illustration of experimentally measured 2D receptive-field profiles of three simple cells in cat striate cortex (top row) obtained in the laboratory of L. A. Palmer and J. P. Jones (University of Pennsylvania Medical School). Each plot shows the excitatory or inhibitory effect of a small flashing light or dark spot on the firing rate of the cell, as a function of the (x, y) location of the stimulus, computed by reverse correlation of the 2D stimulus sequence with the neural-response sequence. The second row shows the best-fitting 2D Gabor function for each cell's receptive-field profile, based on Eqs. (3) with the parameters fitted by least squares. The third row shows the residual error between the measured response profile of each cell and Eqs. (3). In formal statistical tests, the residuals were indistinguishable from random error for 33 of the 36 simple cells tested. (From Ref. 28.)

luminance within their receptive fields by their weighting functions.[21-23] Provided that their discharge threshold is exceeded, simple cells linearly weight the local spatial-luminance distribution by their 2D receptive-field profile, consisting of excitatory and inhibitory influences on the cell's firing frequency. In the classical formulation,[25] the receptive-field profile of a visual neuron is a plot of its relative response to a point of light as a function of the point's location in visual space. Under the condition of linearity, then, the response of a given neuron to an arbitrary image is the 2D integral of the product of its receptive-field profile times the visual image 2D luminance distribution, and the neuron can be treated as a 2D spatial filter.[20]

Unfortunately, virtually the entire body of quantitative reports on simple cells' receptive-field profiles has been 1D. Nonetheless, the existing descriptions are consistent with the filter forms shown in Figs. 1 and 2. The basic receptive-field structure of simple cells consists of several (usually two to five) tapering rows of alternating excitatory and inhibitory subregions,[9,15,23,26] although the early characterizations of Hubel and Wiesel[1,2] described only the central most salient two or three subregions (their bipartite and tripartite cell types). DeValois *et al.*[9] observed that "Quantitative studies of simple-cell receptive fields show them to have a distinctly periodic structure, with additonal side-bands beyond those seen in the initial studies." This periodic tapering structure has recently been more extensively and quantitatively documented.[27]

2D empirical studies of receptive-field profiles, recently completed,[28] have quantitatively confirmed for 30 simple cells in cat visual cortex the appropriateness of the 2D Gabor filter family expressed in Eqs. (3). Novel 2D experimental techniques were developed for inferring a simple cell's response to a small bright or dark spot of light flashed in 256 different (x, y) locations specified by a 16×16 grid covering the cell's receptive field. After some 10,000 randomly positioned stimulus presentations lasting 50 msec each, the recorded neural-firing response train of a given cell was reverse correlated with the stimulus presentation sequence to calculate, for each of the 256 locations, the excitatory or inhibitory effect of the spot of light on the firing probability of the cell. These correlograms, which constitute empirical 2D receptive-field profiles, are shown in Fig. 3 for some of the 36 simple cells so studied. The top row gives the empirical 2D profile for three representative cells, and the second row shows the best-fitting member of Eqs. (3) with parameters estimated by the method of least-squared error by a simplex routine. The residual differences between the best-fitting 2D Gabor filter and the original data surfaces are shown for each cell in the third row. Formal statistical chi-squared tests on whether these residual error surfaces arise from random noise accepted the 2D Gabor filter hypothesis for 33 of the 36 cells studied and rejected it marginally for the remaining 3.

5. SIMPLE-CELL CONSTRAINTS ON DEGREES OF FREEDOM IN THE TWO-DIMENSIONAL GABOR FILTER FAMILY

There are eight degrees of freedom in the 2D Gabor filter family: two coordinates (x_0, y_0) specifying the location of the filter in 2D visual space; two modulation coordinates (u_0, v_0) specifying the location of the filter in 2D frequency space, interpretable as preferred orientation and spatial frequency; the phase of the modulation component, which determines the symmetry–antisymmetry mixture of the filter; and the width and the length of the 2D elliptical Gaussian envelope (a and b), which are reciprocal in the two 2D domains, and the relative angle between the 2D elliptical Gaussian axes and the orientation of the modulation wave vector. Of these eight, the first four (x_0, y_0, u_0, v_0) are the independent variables that form the axes of our information hyperspace and must be spanned in order to pave the space. The phase parameter need take on only two (arbitrary) values in order to specify the coefficient for each location in 4D information hyperspace, and the three remaining Gaussian parameters govern bandwidths and the axes of separability in the sampling scheme.

In this section we discuss apparent physiological constraints on the four free parameters remaining after the filter center coordinates have been specified in the two 2D domains, as far as existing physiological data on populations of simple cells permit.

A. Phase

The fundamental discovery by Pollen and Ronner[17] of adjacent pairs of simple cells matched in preferred spatial frequency and orientation but having a quadrature phase relation (90° phase offset in their response to drifting sine-wave gratings) does not in itself imply that there are preferred or canonical absolute phase angles, such as sine and cosine, relative to receptive-field centers. Although such canonical 1D receptive-field profiles with either pure even or pure odd symmetry are frequently presented,[8,15,21] asymmetric simple-cell receptive fields are known to exist as well.[1,13,23] In the 2D study[28] of receptive-field profiles of 36 simple cells discussed in Section 4 and illustrated in Fig. 3, in which the 2D profiles were fitted by Eqs. (3) with all free parameters, the distribution of best-fitting absolute phases relative to receptive-field centers emerged to be remarkably uniform for the population of cells. Of course, such a uniform distribution of absolute phases, which can be represented by a free additive mixture of pure even and pure odd symmetries, is not incompatible with the Pollen–Ronner finding of quadrature *relative* phases between adjacent cells.

B. Orientation Bandwidths, Spatial-Frequency Bandwidths, and Spatial Dimensions

It is known that neurons in the visual cortex have a broad range of receptive-field dimensions, orientation bandwidths, and spatial-frequency bandwidths. These empirical parameters are statistically correlated in varying degrees with one another and with other variables, such as eccentricity (distance in visual space from the fovea), and with the cell's preferred spatial frequency. Such correlations when strong imply significant constraints on the degrees of freedom of the 2D filter family and may reveal an important underlying logic in the sampling scheme that paves information hyperspace.

DeValois *et al.* report that the positive correlation between cells' orientation bandwidth and spatial-frequency bandwidth is "the largest correlation we found between any of the variables we measured" (Ref. 29, p. 553). The typical values encountered for these bandwidths in cat cortical simple cells are presented statistically in Tables 2 and 3, based on eight independent studies. Clear central tendencies for both bandwidths consistently emerge: The mean of the mean orientation half-bandwidths found in these studies, weighted by the

Table 2. Orientation Bandwidths of Cat Cortical Simple Cells: Half-Width at Half-Response

Mean (deg)	Range (octaves)	N	Ref.
17	8–31	40	30
16.7	7–30	39	31
13.9	5–28	14	32
19.5	7–32	54	33

Weighted mean of the means, 17.5°; total N, 147

Table 3. Spatial-Frequency Bandwidths of Cat Cortical Simple Cells: Full Width at Half-Response

Mean (octaves)	Range (deg)	N	Ref.
1.3	0.7–2.5	184	21
1.2	0.5–2.5	unknown	34
1.3	0.6–1.9	16	23
1.47	0.96–2.4	27	15

Weighted mean of the means; 1.32 octaves; total N, > 227

number of cells in each study, is 17.5° (total N = 147), and the mean of the mean spatial-frequency full bandwidths is 1.32 octaves (total N = 227). Although only data from cat simple cells are summarized in these tables, the existing primate bandwidth statistics are comparable. DeValois *et al.*[29] report that "The median (spatial frequency full-bandwidth) for simple cells (both foveal and parafoveal) is about 1.4 octaves . . ." (N = 225) in the macaque; similarly, their data (Ref. 35, p. 541) for orientation half-bandwidths in the macaque show a median of about 20° (N = 139).

The positive correlation that has been observed[29,36] between orientation bandwidths and spatial-frequency bandwidths of simple cells imposes an important constraint on the joint behavior of the free parameters in Eqs. (3). We noted previously that 2D Gabor filters, which occupy a fixed amount of area in the 2D space domain and hence a fixed amount of 2D frequency-domain area centered on a given modulation frequency, must have an inverse correlation between these two bandwidths. As is indicated in relation (2) and in Figs. 2B and 2C, for such a family with constant area product $(\Delta u)(\Delta v)$, any changes in filter shape that improve orientation resolution will worsen spatial-frequency resolution and vice versa. On the other hand, for a family of filters occupying different amounts of area but preserving a constant spatial aspect ratio $(\Delta x)/(\Delta y)$, and hence also a constant aspect ratio $(\Delta v)/(\Delta u)$ in the 2D frequency domain, the orientation bandwidth and spatial-frequency bandwidth would be positively correlated as observed empirically.

The exact relationship for 2D Gabor filters is worth deriving, for comparison with data and in order to infer parameter constraints. Let us define λ to be the width/length spatial-aspect ratio $(\Delta x)/\Delta y)$ of a 2D Gabor filter; we know from Eqs. (1) that if $(\Delta x)/(\Delta y) = \lambda$, then also $(\Delta v)/\Delta u) = \lambda$. For the canonical filter forms shown in Fig. 2, which have moderate bandwidths and ω_0 modulation wave vectors parallel to the principal axes, we can interpret the height (Δv) of the frequency-domain ellipses geometrically in terms of the filter's orientation half-bandwidth $\Delta\theta_{1/2}$:

$$(\Delta v) = 2\omega_0 \sin(\Delta\theta_{1/2}).$$

Similarly, the spatial-frequency bandwidth (Δu) can be expressed in octaves so that it is commensurate with physiological data. For a filter whose center frequency is ω_0 and whose full bandwidth (in cycles/degree) is (Δu), the full bandwidth expressed in octaves, $\Delta\omega$, is defined as

$$\Delta\omega = \log_2\left[\frac{\omega_0 + (\Delta u)/2}{\omega_0 - (\Delta u)/2}\right],$$

so, in inverted form,

$$(\Delta u) = 2\omega_0\left[\frac{(2^{\Delta\omega} - 1)}{(2^{\Delta\omega} + 1)}\right].$$

Combining these expressions, we arrive at the following relationship between a 2D Gabor filter's spatial width/length aspect ratio λ, orientation half-bandwidth $\Delta\theta_{1/2}$, and spatial-frequency bandwidth $\Delta\omega$ in octaves:

$$\Delta\theta_{1/2} = \arcsin\left[\lambda\,\frac{(2^{\Delta\omega} - 1)}{(2^{\Delta\omega} + 1)}\right]. \quad (4)$$

Equation (4) expresses explicitly the fact that for a fixed spatial aspect ratio λ, there is a positive correlation between spatial-frequency bandwidth and orientation bandwidth. This relationship between bandwidths is independent of the receptive-field modulation frequency ω_0; it is clear from Fig. 2 that if this frequency increases or if the spatial 2D envelope simply expands, then both the orientation bandwidth and the spatial-frequency bandwidth (in octaves) become sharper. The relative payoff of these operations for the two bandwidths is dictated by the spatial-aspect ratio λ. A small λ favors orientation selectivity at the expense of spatial-frequency selectivity, whereas a large λ favors spatial-frequency selectivity at the expense of orientation.

Space-domain measurements of λ in populations of simple cells[28] usually range between 1/4 and 1. In order to fit the observed strong correlation between orientation bandwidth and spatial-frequency bandwidth noted by Movshon,[36] Table 4 has been constructed on the basis of Eq. (4) with λ = 0.6 to show the correlation predicted by such 2D Gabor filters. We note first that the means and the ranges of bandwidths in this table correspond to the actual empirical bandwidth data as summarized in Tables 2 and 3. Table 4 shows that for various 2D Gabor filters whose spatial-frequency bandwidths range from 0.5 to 2.5 octaves and with λ = 0.6, the predicted orientation half-bandwidths increase steadily at the rate of about 10° per octave. This relationship is in striking agreement with that reported empirically by Movshon,[36] who wrote:

Table 4. Predicted Correlation between Orientation Bandwidth and Spatial-Frequency Bandwidth for 2D Gabor Filters with 0.6 Width/Length Spatial Aspect Ratio[a]

Spatial-Frequency Full Bandwidth (octaves)	Orientation Half-Bandwidth (deg)
0.5	5.9
1.0	11.5
1.5	16.7
2.0	21.1
2.5	24.8

[a] From Eq. (4).

"Orientation selectivity and spatial frequency selectivity are well correlated with one another: orientation half-widths increase by about 10 degrees for each octave increase in spatial frequency bandwidth." (N = 114 cells; correlation coefficient r = 0.7.)

Similar experiments in primate visual cortex by DeValois *et al.*[29] report a slightly smaller positive correlation of 0.5 (significant beyond the 0.001 level) between these two variables in 168 macaque striate cortical cells. A two-parameter regression line fitted by least squares (Fig. 8 of Ref. 29) has a slope considerably higher than that reported by Movshon[36] because their intercept parameter was free rather than constrained to go through the origin; consequently, their regression line predicts that a cell with a spatial-frequency bandwidth of 0.4 octave would have infinitely sharp orientation tuning. If their regression line were constrained to have zero intercept, it appears that their data would yield about the same regression slope as Movshon's. In any case, the regression line of DeValois *et al.*[29] is well described (for $\Delta\omega$ between 1 and 2 octaves) by a 2D Gabor filter having a spatial aspect ratio of $\lambda = 1$. When $\Delta\omega$ = 1 octave, Eq. (4) predicts for this 2D Gabor filter that $\Delta\theta_{1/2} = 19°$, and their empirical regression line predicts 17°; when $\Delta\omega$ = 1.5 octave, the Gabor filter predicts $\Delta\theta_{1/2} = 29°$, and their regression line predicts 31°; and when $\Delta\omega$ = 2 octaves, the Gabor filter predicts $\Delta\theta_{1/2} = 37°$, and their regression line predicts 45°.

The variety of orientation bandwidths and spatial-frequency bandwidths encountered suggests that different cells occupy information hyperspace with different strategies, sometimes favoring $\Delta\theta_{1/2}$ at the expense of Δy, sometimes favoring Δx at the expense of $\Delta\omega$, and so on. Presumably these variations represent a division of labor among diverse strategies for extracting different kinds of spatial information subject to the inescapable uncertainty relations [Eqs. (1a) and (b)]. Still, the range[28] of spatial-aspect ratios, typically $1/4 < \lambda < 1$, is relatively narrow when placed in the context of at least a 30:1 range of simple-cell center diameters[29] (even just in the foveal projection), corresponding to a 1000:1 range of receptive-field areas. Interpreting this observation in terms of constraints on the parameters a and b in Eqs. (3), we conclude that the ratio (b/a) is relatively stable, whereas the product ab has an enormous range of at least a thousandfold.

C. Correspondence of Modulation Axis and Envelope Axes

A final empirical constraint on the degrees of freedom in the general family of 2D Gabor filters represented by Eqs. (3) is the relative angle between the modulation wave vector and the principal axes of the elliptical Gaussian envelope. In Figs. 1 and 2 these were always parallel, but this condition is not necessary for achieving the theoretical minimum of joint occupied-area products in the two 2D domains. The 2D spectral consequence of rotating the modulation wave vector relative to the principal axes is a rotation of the elliptical *centroids* around the origin of coordinates of the Fourier plane, without rotation of the ellipses themselves about their centroids. Thus the spectral masses are simply moved (without change of attitude) to the (u_0, v_0) coordinates of the modulation wave vector, as can be understood from the 2D modulation theorem noted in Table 1. In Fig. 2B, for example, noncorrespondence of modulation axes and envelope principal axes would, in the 2D frequency domain, lift the conjugate spectral ellipses above and below the u axis while keeping their major axis parallel to it. Obviously this has a severe consequence: The filter's preferred spatial frequency would depend dramatically on the test component's orientation, and conversely the filter's orientation preference would depend greatly on spatial frequency. To give a concrete example: In Fig. 2 B, oblique modulation within this envelope would rotate the spectral centroids to 45° in the 2D frequency domain, resulting in quite different orientation preferences for different spatial frequencies. Specifically, at the $1/e$ levels of filter sensitivity, the preferred orientation would change from 32° to 66° while the spatial frequency varied over a 0.75-octave range. Conversely, the filter's preferred spatial frequency would change by 0.75 octave while the test orientation spanned this 34° range.

Is such behavior observed neurophysiologically in simple cells? Unfortunately it is not yet possible to answer this question definitively because virtually all investigations have made an implicit assumption of spectral polar separability, namely, that any given cell has a preferred orientation and a preferred spatial frequency that are independent of the value of the other variable. A full 2D spectral characterization,[20] rather than two 1D tuning curves, would be necessary to reveal properties of nonseparability such as that possessed by the 2D Gabor filter in the above example. In the recent investigation[28] employing full 2D spectral methods as well as measuring a full 2D spatial impulse-response function as illustrated in Fig. 3, it was found that for the 36 cat simple cells studied and simplex fitted to Eqs. (3) with all free parameters, only 50% had best-fitting modulation wave vectors within ±10° of the elliptical Gaussian major axis. The remaining 50% showed noncorrespondences at an exponentially decaying rate out to 45°. Although more data concerning this degree of freedom are required, it appears that there is significant tendency for simple cells to have a modulation axis in correspondence with the field axis. The spectral consequence is a tendency for the 2D spectral masses to align radially in the 2D frequency plane (as seen in Fig. 10 of Ref. 29) and thus to keep a cell's preferred orientation relatively independent of spatial frequency.

To summarize: In this section we have noted several major physiological constraints on the degrees of freedom in the proposed 2D Gabor filter family represented by Eqs. (3), in terms of the joint behavior of the parameters a, b, u_o, and v_0 across simple-cell populations. In particular, the orientation bandwidths and spatial-frequency bandwidths that these parameters together govern are constrained by the means and ranges given in Tables 2 and 3. Moreover, the relatively strong positive correlation observed[29,36] between the $\Delta\theta_{1/2}$ and $\Delta\omega$ bandwidths of simple cells (as noted in Table 4) constrains the aspect ratio $\lambda = b/a$ to a relatively small range, whereas the product ab varies over at least a thousandfold range. Finally, based on scantier data, it appears that the absolute phase of simple-cell receptive-field modulation (and hence degree of symmetry) is a rather unconstrained parameter, whereas the axis of modulation is rather more constrained to correspond to the receptive-field envelope axis and thus tends to keep spectral-response regions aligned radially in the 2D frequency plane.

6. CONCLUSIONS

2D linear spatial filters are constrained by general 2D uncertainty relations Eqs. (1a) and (1b), which limit their attainable joint resolution in the 2D space domain and the 2D frequency domain. The family of 2D filters generated by Eqs. (3) optimizes these uncertainty relations and thus achieves the theoretical limit of joint resolution in an information hyperspace whose four axes are interpretable as the two coordinates of visual space plus the polar spectral variables of orientation and spatial frequency. Each such theoretical filter occupies one irreducible quantal volume in the information hyperspace, corresponding to an independent datum, and thus an ensemble of such filters can encode information with optimal efficiency along these four coordinates.

Simple cells in the visual cortex are known to be selective for these four coordinates, each cell having an x, y location in visual space, a preferred orientation, and a preferred spatial frequency. It is well known[1,2] that the first three of these variables are sampled in a systematic way by striate simple cells, and there is evidence[6,29,37] for a systematic sampling of the fourth variable as well. The question arises of the efficiency of such sampling. Previous applications of Gabor theory for addressing this issue in spatial vision have been basically 1D and therefore have not explicitly placed resolution for orientation in the same framework as resolution for spatial frequency and the two dimensions of space-domain resolution. Recent 2D data have been presented here that suggest that the various 2D receptive-field profiles encountered in populations of simple cells are well described by this optimal family of 2D filters.

Deeper constraints appear to limit the degrees of freedom of the 2D filter set actually adopted by linear striate simple cells. The observed ranges of orientation bandwidths and spatial-frequency bandwidths, and the correlation between these two, indicate that the receptive-field width/length aspect ratios are rather tightly constrained (between 1/4 and 1), whereas the field widths and lengths themselves vary over an enormous range. There is a division of labor among simple cells for the resolution of information along the different axes of information hyperspace, some cells, for example, favoring orientation selectivity at the expense of spatial resolution in one direction, and so on. Further constraints evidently act on a cell's field modulation orientation in relation to the receptive field's principal axes, as indicated both by 2D space-domain least-squares fits of the free parameters and by the tendency for the elongated 2D spectral-response regions to align radially in the frequency plane along a polar grid.

The model of early 2D spatial visual representation suggested by this 2D generalization of Gabor's scheme for analyzing temporal signals is one in which polar 2D spectral signatures are extracted within local 2D spatial windows of the retinal image. The original proponents of such an interpretation of visual cortical neurons were Pollen *et al.*,[5] who first hypothesized a local 2D spectral analysis within "restricted regions of visual space." The present formulation of receptive-field organization based on the principle of joint entropy minimization in information hyperspace leads essentially to a formal realization of their concept. The richness of representations based on local spectral signatures is exemplified by the speech spectrogram, in which a spoken sentence is decomposed into format frequency bands within local windows of time (Ref. 38, pp. 142–184).

Important questions remain concerning the sampling strategies adopted by ensembles of simple cells for spanning the four principal tuning variables. The concept of the hypercolumn, introduced by Hubel and Wiesel[1,2] for describing ensembles of neurons that span a complete set of orientation preferences, is suggestive of a modular organization that coarsely embeds the 2D Fourier plane in polar coordinates within each local region of the retinotopic mapping of visual space, which itself has a polar geometry. Understanding the sampling logic of embedding a local polar spectral mapping within the global spatial one will require both further empirical data on joint population properties of cortical neurons and novel theoretical analysis.[39]

ACKNOWLEDGMENTS

I am grateful to S. Marčelja for many useful suggestions, particularly for pointing out that the two 1D uncertainty relations are stronger conditions than the joint 2D version, to J. Jones and L. Palmer for permission to use the unpublished material in Fig. 3, and to R. Kronauer and D. Pollen for helpful discussions. This research was supported by U.S. Air Force Office of Scientific Research contract F49620-81-K-0016.

REFERENCES

1. D. G. Hubel and T. N. Wiesel, "Receptive fields, binocular interaction, and functional architecture in the cat's visual cortex," J. Physiol. (London) **160**, 106–154 (1962).
2. D. G. Hubel and T. N. Wiesel, "Sequence regularity and geometry of orientation columns in the monkey striate cortex," J. Comp. Neurol. **158**, 267–293 (1974).
3. U. Neisser, *Cognitive Psychology* (Prentice-Hall, Englewood Cliffs, N.J., 1967).
4. F. W. Campbell and J. G. Robson, "Application of Fourier analysis to the visibility of gratings," J. Physiol. (London) **197**, 551–566 (1968).
5. D. A. Pollen, J. R. Lee, and J. H. Taylor, "How does the striate cortex begin the reconstruction of the visual world?" Science **173**, 74–77 (1971).
6. L. Maffei and A. Fiorentini, "The visual cortex as a spatial frequency analyzer," Vision Res. **13**, 1255–1267 (1973).
7. D. A. Pollen and J. H. Taylor, "The striate cortex and the spatial analysis of visual space," in *The Neurosciences, Third Study Program*, F. O. Schmitt and F. G. Worden, eds. (MIT, Cambridge, Mass. 1974), pp. 239–247.
8. R. L. DeValois, D. G. Albrecht, and L. G. Thorell, "Cortical cells: bar and edge detectors, or spatial frequency filters," in *Frontiers of Visual Science*, S. J. Cool and E. L. Smith III, eds. (Springer-Verlag, New York, 1978).
9. K. K. DeValois, R. L. DeValois, and E. W. Yund, "Responses of striate cortical cells to grating and checkerboard patterns," J. Physiol. (London) **291**, 483–505 (1979).
10. I. D. G. Macleod and A. Rosenfeld, "The visibility of gratings: spatial frequency channels or bar-detecting units?" Vision Res. **14**, 909–915 (1974).
11. C. W. Tyler, "Selectivity for spatial frequency and bar width in cat visual cortex," Vision Res. **18**, 121–122 (1978).
12. D. G. Albrecht, R. L. DeValois, and L. G. Thorell, "Visual cortical neurons: are bars or gratings the optimal stimuli?" Science **207**, 88–90 (1981).
13. S. Marčelja, "Mathematical description of the responses of simple cortical cells," J. Opt. Soc. Am. **70**, 1297–1300 (1980).
14. D. M. MacKay, "Strife over visual cortical function," Nature **289**, 117–118 (1981).

15. J. J. Kulikowski and P. O. Bishop, "Fourier analysis and spatial representation in the visual cortex," Experientia **37,** 160–163 (1981).
16. D. Gabor, "Theory of communication," J. Inst. Electr. Eng. **93,** 429–457 (1946).
17. D. A. Pollen and S. F. Ronner, "Phase relationships between adjacent simple cells in the visual cortex," Science **212,** 1409–1411 (1981).
18. B. Sakitt and H. B. Barlow, "A model for the economical encoding of the visual image in cerebral cortex," Biol. Cybern. **43,** 97–108 (1982).
19. J. J. Kulikowski, S. Marčelja, and P. O. Bishop, "Theory of spatial position and spatial frequency relations in the receptive fields of simple cells in the visual cortex," Biol. Cybern. **43,** 187–198 (1982).
20. J. G. Daugman, "Two-dimensional spectral analysis of cortical receptive field profiles," Vision Res. **20,** 847–856 (1980).
21. J. A. Movshon, I. D. Thompson, and D. J. Tolhurst, "Spatial summation in the receptive fields of simple cells in the cat's striate cortex," J. Physiol. (London) **283,** 53–77 (1978).
22. J. A. Movshon and D. J. Tolhurst, "On the response linearity of neurons in cat visual cortex," J. Physiol. (London) **249,** 56P–57P (1975).
23. B. W. Andrews and D. A. Pollen, "Relationship between spatial frequency selectivity and receptive field profile of simple cells," J. Physiol. (London) **287,** 163–176 (1979).
24. A. Papoulis, *Systems and Transforms with Applications in Optics* (McGraw-Hill, New York, 1968).
25. R. W. Rodieck, "Quantitative analysis of cat retinal ganglion cell response to visual stimuli," Vision Res. **5,** 583–601 (1965).
26. J. Wilson and S. Sherman, "Receptive field characteristics of neurones in cat striate cortex: changes with visual field eccentricity," J. Neurophysiol. **39,** 512–533 (1976).
27. W. H. Mullikin, J. P. Jones, and L. A. Palmer, "Periodic simple cells in cat area 17," J. Neurophysiol. **52,** 372–387 (1984).
28. J. P. Jones, L. A. Palmer, and J. G. Daugman, "Information management in the visual cortex," Science (to be published).
29. R. L. DeValois, D. G. Albrecht, and L. G. Thorell, "Spatial frequency selectivity of cells in macaque visual cortex," Vision Res. **22,** 545–559 (1982).
30. G. H. Henry, B. Dreher, and P. O. Bishop, "Orientation selectivity of cells in cat striate cortex," J. Neurophysiol. **37,** 1394–1409 (1974).
31. D. Rose and C. Blakemore, "An analysis of orientation selectivity in the cat's visual cortex," Exp. Brain Res. **20,** 1–17 (1974).
32. D. W. Watkins and M. A. Berkley, "The orientation selectivity of single neurons in cat striate cortex," Exp. Brain Res. **19,** 433–446 (1974).
33. P. Heggelund and K. Albus, "Orientation selectivity of single cells in the striate cortex of cat: the shape of orientation tuning curves," Vision Res. **18,** 1067–1071 (1978).
34. D. G. Albrecht, L. G. Thorell, and R. L. DeValois, "Spatial and temporal properties of receptive fields in monkey and cat visual cortex," *Society for Neuroscience, Abstracts* (9th Annual Meeting) (Society for Neuroscience, Atlanta, Ga. 1979), p. 775.
35. R. L. DeValois, E. W. Yund, and N. Hepler, "The orientation and direction selectivity of cells in macaque visual cortex," Vision Res. **22,** 531–544 (1982).
36. J. A. Movshon, "Two-dimensional spatial frequency tuning of cat striate cortical neurons," *Society for Neuroscience, Abstracts* (9th Annual Meeting) (Society for Neuroscience, Atlanta, Ga., 1979), p. 799.
37. R. Tootell, M. Silverman, and R. L. DeValois, "Spatial frequency columns in primary visual cortex," Science **214,** 813–815 (1981).
38. J. L. Flanagan, *Speech Analysis, Synthesis, and Perception,* 2nd ed. (Springer-Verlag, Berlin, 1972).
39. H. Stark, "Sampling theorems in polar coordinates," J. Opt. Soc Am. **69,** 1519–1525 (1979).

John G. Daugman

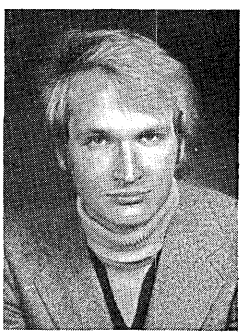

John G. Daugman was born in 1954 and educated at Harvard University, receiving the B.A. degree in physics in 1976 and the Ph.D. degree in psychology in 1983. Subsequently he was a postdoctoral fellow in biomedical physics at Harvard and is currently a visiting scientist at Ludwig-Maximilians-Universität in Munich, Federal Republic of Germany. His major research interests concern biological and artificial means of image representation and processing, including neural-encoding principles, semantic image decomposition, and epistemological theories of representation. He was the designer of the Innisfree image synthesizer, currently used in more than 100 research institutes in 15 countries. Starting in autumn 1985, he will join the faculty at Harvard with a joint appointment as assistant professor of psychology and of electrical engineering and computer science.